HHS Public Access

Author manuscript

Nature. Author manuscript; available in PMC 2010 June 17.

Published in final edited form as:

Nature. 2009 December 17; 462(7275): 930–934. doi:10.1038/nature08677.

E2F1-3 Switch from Activators in Progenitor Cells to Repressors in Differentiating Cells

Jean-Leon Chong[1,2,3,†], **Pamela L. Wenzel**[1,2,3,†,¶], **M. Teresa Sáenz-Robles**[4,†], **Vivek Nair**[1,2,3], **Antoney Ferrey**[1,2,3], **John P. Hagan**[1,3], **Yorman M. Gomez**[1,2,3], **Nidhi Sharma**[1,2,3], **Hui-Zi Chen**[1,2,3], **Madhu Ouseph**[1,2,3], **Shu-Huei Wang**[1,2,3], **Prashant Trikha**[1,2,3], **Brian Culp**[1,2,3], **Louise Mezache**[1,2,3], **Douglas J. Winton**[5], **Owen J. Sansom**[6], **Danian Chen**[7], **Rod Bremner**[7], **Paul G. Cantalupo**[4], **Michael L. Robinson**[8], **James M. Pipas**[4], and **Gustavo Leone**[1,2,3,*]

[1] Department of Molecular Virology, Immunology and Medical Genetics, College of Medicine, The Ohio State University, Columbus, OH 43210, USA

[2] Department of Molecular Genetics, College of Biological Sciences, The Ohio State University, Columbus, OH 43210, USA

[3] Comprehensive Cancer Center, The Ohio State University, Columbus, OH 43210, USA

[4] Department of Biological Sciences, University of Pittsburgh, Pittsburgh PA 15260

[5] Cambridge Research Institute, Li Ka Shing Centre, Cambridge CB2 ORE, UK

[6] The Beatson Institute for Cancer Research, Glasgow G611BD, UK

[7] Toronto Western Research Institute, University Health Network, Departments of Ophthalmology and Visual Science, and Laboratory Medicine and Pathobiology, University of Toronto, Ontario, Canada. M5T 2S8

[8] Department of Zoology, Miami University, Oxford, Ohio 45056, USA

Abstract

In the classic paradigm of mammalian cell cycle control, Rb functions to restrict cells from entering S phase by sequestering E2F activators (*E2f1*, *E2f2* and *E2f3*), which are invariably

[*]Corresponding Author Information: Gustavo Leone, Human Cancer Genetics Program, Department of Molecular Virology, Immunology and Medical Genetics, Department of Molecular Genetics, The Ohio State University, Comprehensive Cancer Center, 460 W. 12th Ave., Room 808, Columbus, OH 43210, Telephone: 614-688-4567, FAX: 614-688-4181, Gustavo.Leone@osumc.edu.

[†]These authors contributed equally to this work

[¶]*Current address*: Division of Pediatric Hematology/Oncology, Children's Hospital Boston; Department of Biological Chemistry and Molecular Pharmacology, Harvard Medical School, Boston, MA 02115

Author Contributions. M.L.R., J.M.P. and G.L. designed and supervised this study, analyzed data, and helped write and edit the manuscript. J-L.C., P.L.W. and M.T.S. designed and performed experiments, collected and analyzed data, and co-wrote the paper. V.N., A.F., Y.M.G., N.S., H-Z.C., M.O., S-H.W., P.T., B.C. and L.M. technically assisted with experiments and collected and analyzed data. D.C. and R.B. performed and analyzed gene expression of retina. J.P.H. and P.G.C. contributed to the analysis and comparison of gene microarray data. D.J.W. and O.J.S. contributed to the generation of key reagents.

Author information. All microarray data has been deposited to the Gene Expression Omnibus at the National Center for Biotechnology Information under accession numbers GSE16454. Reprints and permissions information is available at ww.nature.com/reprints.

portrayed as the ultimate effectors of a transcriptional program that commit cells to enter and progress through S phase1, 2. Using a panel of tissue-specific *cre*-transgenic mice and conditional *E2f* alleles we examine the effects of *E2f1*, *E2f2* and *E2f3* triple deficiency in murine ES cells, embryos and small intestines. We show that in normal dividing progenitor cells E2F1-3 function as transcriptional activators, but contrary to current dogma, are dispensable for cell division and instead are necessary for cell survival. In differentiating cells they function in complex with Rb as repressors to silence E2F targets and facilitate exit from the cell cycle. The inactivation of *Rb* in differentiating cells resulted in a switch of E2F1-3 from repressors to activators, leading to the superactivation of E2F responsive targets and ectopic cell divisions, and loss of *E2f1-3* completely suppressed these phenotypes. This work contextualizes the activator versus repressor functions of E2F1-3 *in vivo*, revealing distinct roles in dividing versus differentiating cells and in normal versus cancer-like cell cycles *in vivo*.

Keywords

Small intestine; cell cycle; E2F; retinoblastoma; tumor suppressor

E2Fs function as transcription factors, with E2F1-3 as activators and E2F4-8 as repressors3–8. Although it is a maxim of mammalian cell cycle regulation that the E2F1-3 activator subclass is required for cell proliferation, the evidence for this is based almost exclusively on *in vitro* studies using cells derived from murine and human tissues or on the *in vivo* analysis of *Rb* mutant mice1, 2. Other experiments, however, suggest that these E2Fs can also function as repressors in complex with Rb9–11, yet the relative contribution of activation version repression and the physiological contexts in which these contrary E2F functions are employed remain unclear.

To explore the functions of the E2F activator subclass, we derived $E2f1^{-/-};E2f2^{-/-};E2f3^{LoxP/-}$ ES cells (Supplementary Fig. 1a, 1b) and compared the consequences of inactivating the conditional $E2f3^{LoxP}$ allele in these cells versus in $E2f1^{-/-};E2f2^{-/-};E2f3^{LoxP/LoxP}$ MEFs. The expression of *E2f1*, *E2f2* and *E2f3* in wild type ES cells was generally higher than in MEFs and the loading of E2F3 protein on classic E2F target promoters was comparable between the two proliferating cell types (Supplementary Fig. 2a-c). Consistent with previous observations, the ablation of *E2f1-3* in MEFs with standard *cre*-expressing vectors led to the induction of p53 activity, the loading of E2F4-p130 repressor complexes on E2F target promoters and a marked decrease in E2F target expression (Fig. 1a, Supplementary Fig. 3a–c)5–7. Consequently, triply deficient MEFs underwent a complete cell cycle arrest (Fig. 1b)5–7. In contrast, $E2f1^{-/-};E2f2^{-/-};E2f3^{\Delta/-}$(*TKO*) ES cells failed to activate p53 or form E2F4/p130 repressive complexes, and as a result, E2F target expression was unaffected and cells proliferated equally well as $E2f1^{-/-};E2f2^{-/-};E2f3^{LoxP/-}$ (*DKO*) control cells (Supplementary Fig. 3a-c).

We then evaluated whether triply-deficient ES cells could proliferate *in vivo*. Subcutaneous injection of *TKO* ES cells into athymic nude mice yielded efficient teratoma formation, producing mesoderm, endoderm, and ectoderm at a rate similar to *DKO* ES lines (Fig. 1c, Supplementary Fig. 4a, 4b). Moreover, from $E2f1^{+/-};E2f2^{-/-};E2f3^{+/-}$ intercrosses we

recovered the expected number of live *TKO* embryos as late as E9.5, but none were recovered past E11.5 (Fig. 1d, and data not shown). The live E9.5 *TKO* embryos appeared morphologically normal by gross and histological examination (Fig. 1e and data not shown). While cell proliferation was normal in most tissues, there was evidence of decreased proliferation and increased apoptosis in the myocardium and the first branchial arch of *TKO* embryos (Supplementary Fig. 5a–d). These latter observations are consistent with heart defects found in *E2f3* singly-deleted adult mice12.

To explore whether E2F1-3 might have cell cycle-related functions in tissues that arise later in embryonic and postnatal development, we exploited the highly organized cellular architecture of the small intestine. Maintenance of structural and functional integrity of the small intestine requires continuous epithelial regeneration13. Intestinal stem cells are housed at the base of crypts of Lieberkühn and give rise to transit-amplifying cells. As these cells migrate up from the base and into the finger-like extensions called villi, they exit the cell cycle and differentiate13. Western blot assays showed that *E2f1*, *E2f2* and both isoforms of *E2f3* (E2F3a and E2F3b) are expressed in the crypt and villus (Supplementary Fig. 6). We used *Ah-cre* mice14 to ablate *E2f1-3* in the small intestine *in utero* or in adult mice (*Ah-cre;E2f1*$^{-/-}$*;E2f2*$^{-/-}$*;E2f3*$^{LoxP/LoxP}$, *TKO*). Induction of *Ah-cre* expression by intraperitoneal injection of β-napthoflavone (β-NF) led to the efficient deletion of *E2f3*^{LoxP} in crypt stem cells and transit-amplifying cells by one day post-injection, and in the entire intestinal epithelium within 3–4 days (crypt and villus; Supplementary Fig. 7a–c). Loss of *E2f1-3* did not result in a compensatory increase of other E2F family members, except for a modest increase in *E2f8* (Supplementary Fig. 7d). Whether *E2f3*^{LoxP} was deleted *in utero* at E15.5 or in the adult at 2 months of age, the architecture of *TKO* small intestines remained relatively intact and animals were asymptomatic for 90 days following β-NF administration (Fig. 2a, Supplementary Fig. 8a, 8b). Cell-type specific marker analysis demonstrated that all differentiated epithelial cell-types were appropriately represented in *TKO* small intestines (Fig. 2b, Supplementary Fig. 9). Remarkably, cell proliferation was identical in *TKO* and *control* intestines (Fig. 2c), however, we noted a marked increase in γ-H2AX and P-ATM^{1981} staining in *TKO* crypts and villi (Fig. 2d, 2e, Supplementary Fig. 10a). A parallel analysis of retinal (*Chen et al*, accompanying manuscript) and lens (P.W. unpublished observations) progenitors also revealed increased γ-H2AX staining in *TKO* samples (Supplementary Fig. 10b, 10c). Together, these observations suggest that counter to current dogma, E2F1-3 are dispensable for the proliferation of embryonic stem cells and their mesodermal, endodermal, and ectodermal derivatives, and cells in at least some adult tissues.

Close examination of H&E-stained slides revealed increased numbers of pyknotic nuclei in *TKO* crypts (data not shown). TUNEL and cleaved caspase-3 assays confirmed the presence of apoptotic cells in crypts of *TKO* intestines (Fig. 2f). We also observed increased p53 immunoreactivity in *TKO* crypts (Supplementary Fig. 11a), which was reminiscent of previous work showing exquisite sensitivity of this cellular compartment to oncogene- and radiation-induced p53 responses15. While p53 was elevated in *TKO* crypts, we failed to detect any significant increase in the expression of p53-responsive genes and moreover, the conditional ablation of *p53* (*Ah-cre;E2f1*$^{-/-}$*;E2f2*$^{-/-}$*;E2f3*$^{LoxP/LoxP}$*;p53*$^{LoxP/LoxP}$) did not

suppress the apoptosis caused by *E2f1-3* deficiency (Supplementary Fig. 11b, 11c). Together, these surprising observations suggest that E2F1-3 are dispensable for cell division in the adult and that at least in the small intestine, they function in a p53-independent manner to maintain DNA integrity and cell survival.

To understand the underlying mechanism for these unexpected results, we isolated crypt and villus cell populations from *control* and *E2f1-3*-deficient (*TKO*) small intestines and analyzed global gene expression profiles. Sample preparation and processing of the Affymetrix oligo-arrays are described in the Methods section. We utilized an unbiased method similar to Gene Set Enrichment Analysis to identify genes that were differentially expressed16. Two variables contributed to the observed gene expression changes, cell compartment (crypt vs. villus) and genotype (*TKO* vs. *control*). The cell compartment analysis compared gene expression in crypts and villi of the same genotype (Fig. 3a). For *control* small intestines, this revealed that among the ~45K genes queried, 1207 genes were upregulated and 2363 genes were downregulated as progenitor cells in the crypt migrated up into the villus and exited the cell cycle (>1.5-fold, $p<0.0001$; Supplementary Fig. 12a, Supplementary Table 1). As expected, the expression of most known E2F targets, as defined by previous gene expression17, reporter and chromatin immunoprecipitation assays18 (Supplementary Fig. 12b), was markedly higher in *control* crypts than in associated villi (Fig. 3a, left panel), consistent with the proliferative status of crypts. For *TKO* small intestines, the expression of E2F targets in crypts was only marginally higher than in their associated villi (Fig. 3a, right panel), suggesting that expression of these genes were either reduced in crypts, elevated in villi, or both.

The genotype analysis compared gene expression in *TKO* vs. *control* samples of the same cell compartment. This comparison revealed a modest but significant downregulation of E2F targets in progenitor cells of *TKO* crypts, which included many but not all known classic targets such as *Cdc6*, *Cyclin A2*, *Cyclin E2*, *Top2*, and *Hmgb2* (Fig. 3b–c, left panels, Supplementary Fig. 13a). We suspect that continued proliferation of *TKO* progenitors in the small intestine when E2F targets are limiting likely contributes to replicative stress, DNA damage and the observed increase in γ-H2AX labeling in these cells. Whether these aberrant processes are linked to the death of *TKO* progenitor cells remains to be rigorously evaluated. The genotype comparison also revealed a remarkable upregulation of a large number of E2F targets in differentiated cells of the *TKO* villus (Fig. 3b–c, right panels, Supplementary Fig. 13a). Western blot assays and IF staining showed that the accumulation of two of these E2F target gene products, Mcm3 and Pcna, was widespread throughout the *TKO* villus (Fig. 3d, Supplementary Fig. 13b). Similarly, there was increased expression of E2F targets in differentiated *TKO* cells of the retina and lens (Supplementary Fig. 13c; PW unpublished observations), suggesting a general role for E2F1-3 in transcriptional repression in post-mitotic cells *in vivo*. Chromatin immunoprecipitation (ChIP) assays using villus-enriched lysates derived from *control* and *TKO* small intestines showed that E2F3 occupies E2F binding sites on classic E2F-target promoters (Fig. 3e). Importantly, coimmunoprecipitation assays using intestinal epithelial cells derived from $E2f3^{-/-}$, $E2f3a^{-/-}$ and $E2f3b^{-/-}$ villi showed that both E2F3a/b isoforms19–21 participate in a complex with the Rb protein (Fig. 3f). Consistent with this, Rb was found to be hypophosphorylated in the villus

(Supplementary Fig. 14a). Together, these data suggest that E2F1-3 act as transcription activators in dividing progenitors, and as repressors (in complex with Rb) in differentiating cells of the small intestine.

On the surface, the observation that E2F1-3 repress E2F targets and are dispensable for cell proliferation contradict previous findings from the analysis of *Rb*/*E2f* double knockout animals1, 2, 8. Therefore, to thoroughly explore the mechanistic relationship between Rb and E2F1-3, we used the small intestine as an *in vivo* system where results could be uniformly compared across different genetic configurations. The *Ah*-cre mediated inactivation of *Rb in utero* or in adult mice resulted in increased proliferation of cells in the villus compartment but not in the crypt (Fig. 4a, 4b, Supplementary Fig. 14b–e), indicating that *Rb*-deleted transit-amplifying cells failed to appropriately exit the cell cycle. There was, however, no concomitant increase in apoptosis or defect in cell differentiation (Supplementary Fig. 15a, 15b), and as a result, *Rb*-deficient villi appeared uniformly hyperplastic. The combined ablation of the three *E2fs* completely suppressed the unscheduled proliferation and hyperplasia caused by *Rb* deficiency (*QKO*; Fig. 4a, 4b, Supplementary Fig. 16a). Importantly, the basal levels of proliferation in *QKO* crypts were indistinguishable from control or *TKO* samples (Supplementary Fig. 16b), consistent with the rather normal development of *E2f1-3* deficient small intestines containing an intact *Rb* gene.

The selective requirement for *E2f1-3* in the proliferation of *Rb*-deficient cells provided an opportunity to dissect possible cancer-specific mechanisms of E2F in cell cycle control. We therefore compared global gene expression programs in *control*, *RbKO*, *TKO* and *QKO* intestinal epithelia. Several important insights came from this analysis. First, there were expansive gene expression differences between *control* and *RbKO* villi (1290 upregulated and 487 downregulated genes; Fig. 4c, Supplementary Table 2), but relatively minor differences in their associated crypts (Supplementary Fig. 17a, 17b). Gene Ontology algorithms22 identified a bias for differentially expressed genes involved in the regulation of transcription, DNA metabolic processes and cell cycle (Supplementary Table 3). IF and quantitative RT-PCR assays confirmed the dramatic accumulation of most E2F-target genes in *RbKO* villi (Supplementary Fig. 17c–d). From these data we conclude that *Rb* is critical for the repression of E2F targets at a time when progenitor cells commit to exit the cell cycle and terminally differentiate. Second, hierarchical clustering of all data sets showed that *TKO* and *QKO* tissues clustered together in a separate group from *control* and *RbKO* tissues (Supplementary Fig. 18), suggesting that some functions coordinated by E2F1-3 may be Rb-independent. Finally and most importantly, the expression levels of E2F targets in *TKO* and *QKO* villi were equivalent, and while higher than in *control* villi, they were substantially lower than in *RbKO* villi (Fig. 4c). Quantitative RT PCR assays confirmed the relative expression of E2F targets to be: *control* < *TKO* = *QKO* ≪ *RbKO* (Fig. 4d). From these data, we conclude that the supra-elevated expression of E2F targets observed in *RbKO* villi is due to both ‘derepression’ (lacking intact Rb/E2F1-3 repressor complexes) and E2F1-3 mediated ‘hyper-activation’. In the absence of E2F1-3 mediated hyper-activation, cells in *QKO* villi fail to hyper-activate and thus do not accumulate sufficient levels of E2F targets to undergo

'ectopic' cell proliferation (this threshold level of expression is illustrated as a red dotted line in Fig. 4d).

We provide overwhelming evidence showing that normal cell proliferation in mice can be maintained in the absence of activator E2Fs. We conclude that E2F1-3, like G_1 Cdk's23–25, are not as critical for normal cell proliferation in mammals as original studies implied3, 4, 26–29. However, not all is well in the absence of E2F1-3, since *TKO* dividing progenitors in the small intestine undergo apoptosis. A prosurvival role for E2F1-3 was also evident in retinal progenitor cells of the mouse (*Chen et al*., accompanying paper), however, in the retina cell death was p53 dependent whereas in the small intestine it was p53 independent. Thus, the sensitivity of cells to p53 activation varies considerably across tissue types.

The findings presented here also expose dual functions for E2F1-3 in transcription activation and repression *in vivo*. In dividing progenitor cells, when Rb is inactive (hyperphosphorylated), free E2F1-3 are employed to optimally activate the expression of target genes. The inability to do so in *E2f1-3* deficient tissues still permits cells to replicate their DNA and divide, but at the cost of increased DNA damage and cell death. As cells commit to a terminally differentiated fate, P-Rb is dephosphorylated and forms a physical complex with E2F1-3 proteins. We propose that this is not to just sequester E2F activators but rather, to form the first repressive complex that is necessary to downregulate E2F targets and usher transit-amplifying cells out of the cell cycle. Once cells exit the cell cycle, other professional repressor complexes accumulate, including p130/E2F4 and p107/E2F4, to more permanently enforce the repression of E2F targets. Given that inactivation of *Rb*, but not *p*107 or *p130*30, induces ectopic cell divisions in the small intestine, we suggest that Rb has a unique role in transit-amplifying cells that is dependent on its ability to associate with E2F1-3. Maintenance of quiescence in terminally differentiated cells of the villus, however, is a function that is shared among all members of the Rb family30. In summary, this work challenges the current paradigm of cell cycle control and provides, for the first time, a unified molecular view of how the dual functions of E2F1-3 in transcriptional activation and repression are employed *in vivo* to control normal versus *Rb*-mutant or cancer cell cycles.

METHODS SUMMARY

Mice (*E2f1*$^{-/-}$, *E2f2*$^{-/-}$, *E2f3*$^{f/f}$, *Ah-cre* and *Rb*$^{f/f}$) used for the studies were in mixed background (129SvEv, C57BL/6NTac and FVB/NTac). β-napthoflavone (sigma; N3633-5G) was administered into 2 month old *Ah-cre* mice three times within 24 hours as described previously14 and mice were harvested 7 or 90 days later. β-napthoflavone was also injected into pregnant female mice at 15.5 days postcoitum for analysis of embryos at E18.5. Villus and crypt fractions were isolated as previously described8. Three independent samples from each genetic group were used for gene expression analysis by Affymetrix microarray. Analysis of gene expression data were performed using BRB-array tools developed by Dr. Richard Simon and Amy Peng Lam of the National Cancer Institute. Gene Ontologies were predicted by DAVID (Database for Annotation, Visualization and Integrated Discovery) Bioinformatics Resources at the National Institute of Allergy and Infectious diseases, NIH. X-gal staining, real-time RT-PCR, BrdU, ChIP and TUNEL assays were performed as previously described8, 19. Primers for ChIP, real-time RT-PCR and

genotyping are listed in Supplementary Fig. 19a-b. Antibodies used for Western blot or immunohistochemical staining are listed in Supplementary Fig. 19c.

Supplementary Material

Refer to Web version on PubMed Central for supplementary material.

Acknowledgments

We thank L. Rawahneh and J. Moffitt and R. Rajmohan for excellent technical assistance with histology. We also thank A. de Bruin and S. Naidu for assistance in analyzing histological slides. We are thankful to Drs. Joanna Groden, Mandy Simcox and Denis Guttridge for their critical comments. This work was funded by NIH grants to G.L. (R01CA85619, R01CA82259, R01HD04470, P01CA097189) and NIH grant to J.M.P. (CA098956); J.-L.C. is the recipient of a DoD award (BC061730). P.L.W. was supported by NIH training grant 5 T32 CA106196-04.

References

1. Iaquinta PJ, Lees JA. Life and death decisions by the E2F transcription factors. Curr Opin Cell Biol. 2007; 19:649–657. [PubMed: 18032011]
2. Dimova DK, Dyson NJ. The E2F transcriptional network: old acquaintances with new faces. Oncogene. 2005; 24:2810–2826. [PubMed: 15838517]
3. DeGregori J, Leone G, Miron A, Jakoi L, Nevins JR. Distinct roles for E2F proteins in cell growth control and apoptosis. Proc Natl Acad Sci U S A. 1997; 94:7245–7250. [PubMed: 9207076]
4. Johnson DG, Schwarz JK, Cress WD, Nevins JR. Expression of transcription factor E2F1 induces quiescent cells to enter S phase. Nature. 1993; 365:349–352. [PubMed: 8377827]
5. Wu L, et al. The E2F1-3 transcription factors are essential for cellular proliferation. Nature. 2001; 414:457–462. [PubMed: 11719808]
6. Timmers C, et al. E2f1, E2f2, and E2f3 control E2F target expression and cellular proliferation via a p53-dependent negative feedback loop. Mol Cell Biol. 2007; 27:65–78. [PubMed: 17167174]
7. Sharma N, et al. Control of the p53-p21CIP1 Axis by E2f1, E2f2, and E2f3 is essential for G1/S progression and cellular transformation. J Biol Chem. 2006; 281:36124–36131. [PubMed: 17008321]
8. Saenz-Robles MT, et al. Intestinal hyperplasia induced by simian virus 40 large tumor antigen requires E2F2. J Virol. 2007; 81:13191–13199. [PubMed: 17855529]
9. Rowland BD, Bernards R. Re-evaluating cell-cycle regulation by E2Fs. Cell. 2006; 127:871–874. [PubMed: 17129771]
10. Murga M, et al. Mutation of E2F2 in mice causes enhanced T lymphocyte proliferation, leading to the development of autoimmunity. Immunity. 2001; 15:959–970. [PubMed: 11754817]
11. Iglesias A, et al. Diabetes and exocrine pancreatic insufficiency in E2F1/E2F2 double-mutant mice. J Clin Invest. 2004; 113:1398–1407. [PubMed: 15146237]
12. Cloud JE, et al. Mutant mouse models reveal the relative roles of E2F1 and E2F3 in vivo. Mol Cell Biol. 2002; 22:2663–2672. [PubMed: 11909960]
13. van der Flier LG, Clevers H. Stem Cells, Self-Renewal, and Differentiation in the Intestinal Epithelium. Annu Rev Physiol. 2008
14. Ireland H, et al. Inducible Cre-mediated control of gene expression in the murine gastrointestinal tract: effect of loss of beta-catenin. Gastroenterology. 2004; 126:1236–1246. [PubMed: 15131783]
15. Coopersmith CM, Gordon J. I gamma-Ray-induced apoptosis in transgenic mice with proliferative abnormalities in their intestinal epithelium: re-entry of villus enterocytes into the cell cycle does not affect their radioresistance but enhances the radiosensitivity of the crypt by inducing p53. Oncogene. 1997; 15:131–141. [PubMed: 9244349]
16. Mootha VK, et al. PGC-1alpha-responsive genes involved in oxidative phosphorylation are coordinately downregulated in human diabetes. Nat Genet. 2003; 34:267–273. [PubMed: 12808457]

17. Kong LJ, Chang JT, Bild AH, Nevins JR. Compensation and specificity of function within the E2F family. Oncogene. 2007; 26:321–327. [PubMed: 16909124]
18. Xu X, et al. A comprehensive ChIP-chip analysis of E2F1, E2F4, and E2F6 in normal and tumor cells reveals interchangeable roles of E2F family members. Genome Res. 2007; 17:1550–1561. [PubMed: 17908821]
19. Chong JL, et al. E2f3a and E2f3b contribute to the control of cell proliferation and mouse development. Mol Cell Biol. 2009; 29:414–424. [PubMed: 19015245]
20. Leone G, et al. E2F3 activity is regulated during the cell cycle and is required for the induction of S phase. Genes Dev. 1998; 12:2120–2130. [PubMed: 9679057]
21. Leone G, et al. Identification of a novel E2F3 product suggests a mechanism for determining specificity of repression by Rb proteins. Mol Cell Biol. 2000; 20:3626–3632. [PubMed: 10779352]
22. Eisen MB, Spellman PT, Brown PO, Botstein D. Cluster analysis and display of genome-wide expression patterns. Proc Natl Acad Sci U S A. 1998; 95:14863–14868. [PubMed: 9843981]
23. Malumbres M, Barbacid M. Mammalian cyclin-dependent kinases. Trends Biochem Sci. 2005; 30:630–641. [PubMed: 16236519]
24. Martin A, et al. Cdk2 is dispensable for cell cycle inhibition and tumor suppression mediated by p27(Kip1) and p21(Cip1). Cancer Cell. 2005; 7:591–598. [PubMed: 15950907]
25. Malumbres M, et al. Mammalian cells cycle without the D-type cyclin-dependent kinases Cdk4 and Cdk6. Cell. 2004; 118:493–504. [PubMed: 15315761]
26. Russell P, Nurse P. Schizosaccharomyces pombe and Saccharomyces cerevisiae: a look at yeasts divided. Cell. 1986; 45:781–782. [PubMed: 3518949]
27. Helin K, et al. A cDNA encoding a pRB-binding protein with properties of the transcription factor E2F. Cell. 1992; 70:337–350. [PubMed: 1638634]
28. Kaelin WG Jr, et al. Expression cloning of a cDNA encoding a retinoblastoma-binding protein with E2F-like properties. Cell. 1992; 70:351–364. [PubMed: 1638635]
29. Nevins JR. Transcriptional regulation. A closer look at E2F. Nature. 1992; 358:375–376. [PubMed: 1641018]
30. Haigis K, Sage J, Glickman J, Shafer S, Jacks T. The related retinoblastoma (pRb) and p130 proteins cooperate to regulate homeostasis in the intestinal epithelium. J Biol Chem. 2006; 281:638–647. [PubMed: 16258171]

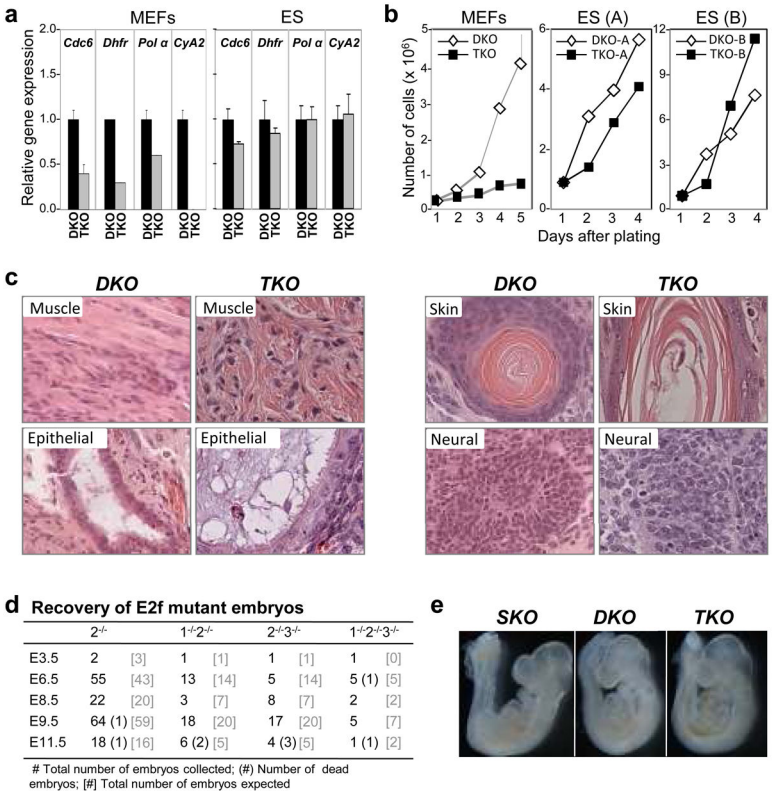

	$2^{-/-}$		$1^{-/-}2^{-/-}$		$2^{-/-}3^{-/-}$		$1^{-/-}2^{-/-}3^{-/-}$	
E3.5	2	[3]	1	[1]	1	[1]	1	[0]
E6.5	55	[43]	13	[14]	5	[14]	5 (1)	[5]
E8.5	22	[20]	3	[7]	8	[7]	2	[2]
E9.5	64 (1)	[59]	18	[20]	17	[20]	5	[7]
E11.5	18 (1)	[16]	6 (2)	[5]	4 (3)	[5]	1 (1)	[2]

Total number of embryos collected; (#) Number of dead embryos; [#] Total number of embryos expected

Figure 1. Cell proliferation in the absence of *E2f1-3*

a Expression of E2F-regulated genes was measured by real-time RT-PCR in proliferating ES and MEFs cells with the indicated genotypes (primer information is provided in Supplementary Fig. 19). **b.** Growth curves of two sets of *DKO* and *TKO* ES cell clones (A and B) and *DKO* and *TKO* MEFs. **c.** *DKO* and *TKO* ES cells were injected underneath the skin of athymic nude mice and teratomas were harvested, sectioned and stained with H&E. Representative tissues of *DKO* and *TKO* teratomas include muscle (mesoderm), respiratory epithelium (endoderm), skin and neural cells (ectoderm). **d.** Embryos derived from intercrosses between $E2f1^{+/-};E2f2^{-/-};E2f3^{+/-}$ mice were collected at various timepoints during pregnancies. **e.** Representative E9.5 embryos were photographed immediately upon collection; $E2f2^{-/-}$ (*SKO*), $E2f2^{-/-};E2f3^{-/-}$ (*DKO*), and $E2f1^{-/-}E2f2^{-/-}E2f3^{-/-}$ (*TKO*) embryos.

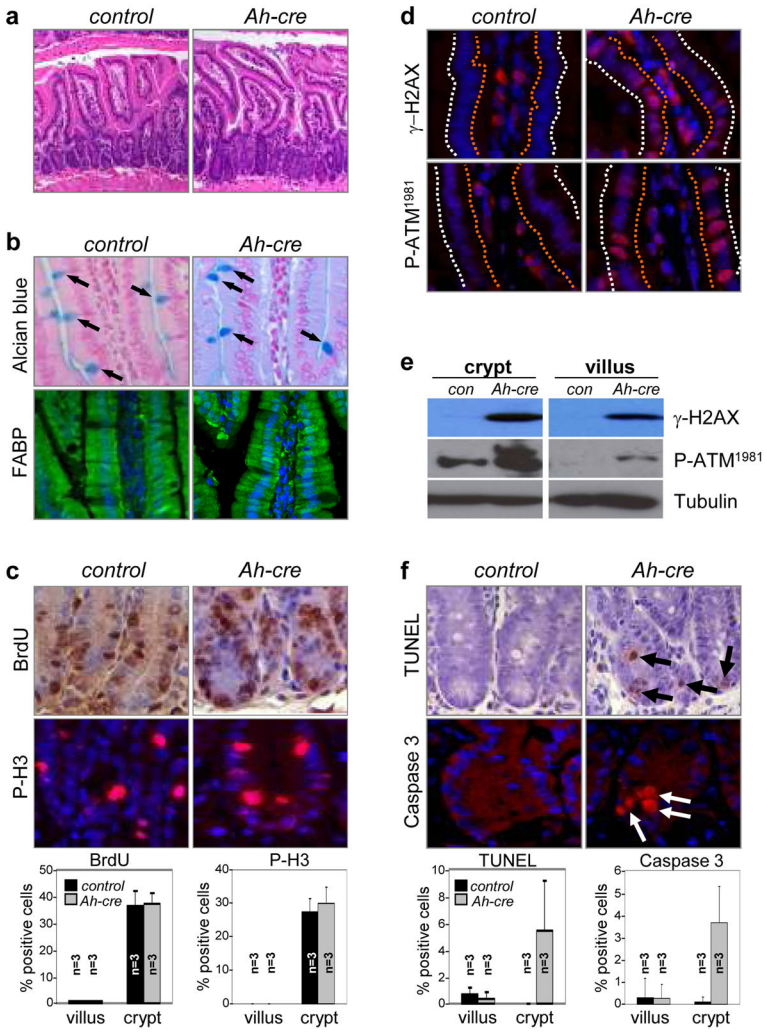

Figure 2. Apoptosis of crypt intestinal cells in the absence of E2f1, E2f2, and E2f3

a H&E stained sections from E2f1$^{-/-}$;E2f2$^{-/-}$;E2f3$^{LoxP/LoxP}$ (control) and Ah-cre;E2f1$^{-/-}$;E2f2$^{-/-}$;E2f3$^{LoxP/LoxP}$ (Ah-cre) intestines after 90 days of β-NF administration. **b**. Analysis of cell differentiation in control and Ah-cre small intestines. Goblet cells were identified by Alcian blue staining (arrows point to positive-stained goblet cells); absorptive cells were identified by anti-Fatty acid binding protein (FABP, green) antibodies; DAPI (blue) was used for staining nuclei. **c.** BrdU (brown) and phosphorylated histone H3 (P-H3, red) immunohistochemical staining was performed on small intestine sections from β-NF injected control and Ah-cre mice. Quantification of BrdU- and phosphorylated histone H3-positive cells in crypts and villi. n=3, 3 different animals with the indicated genotypes were analyzed (bottom panels); error bars indicate standard deviation. **d**. Immunohistochemical staining for γ-H2AX, P-ATM^{1981} in *control* and *Ah-cre* intestinal crypts and villi. The orange dotted line outlines the luminal side of the villus; the white dotted line outlines the outer side of the villus. DAPI (blue) was used for staining nuclei. **e**. Examination of γ-H2AX and P-ATM^{1981} in cell extracts from *control* and *Ah-cre* intestinal crypts and villi by Western blot assays. **f**. Sections of small intestines from β-NF injected *control* and *Ah-cre*

mice were processed for TUNEL (brown) and cleaved caspase-3 (red) assays. DAPI (blue) or hematoxylin was used for staining nuclei. Quantification of TUNEL and cleaved caspase-3 positive cells in crypts and villi (bottom panels). n=3, 3 different animals with the indicated genotypes were analyzed; error bars indicate standard deviation.

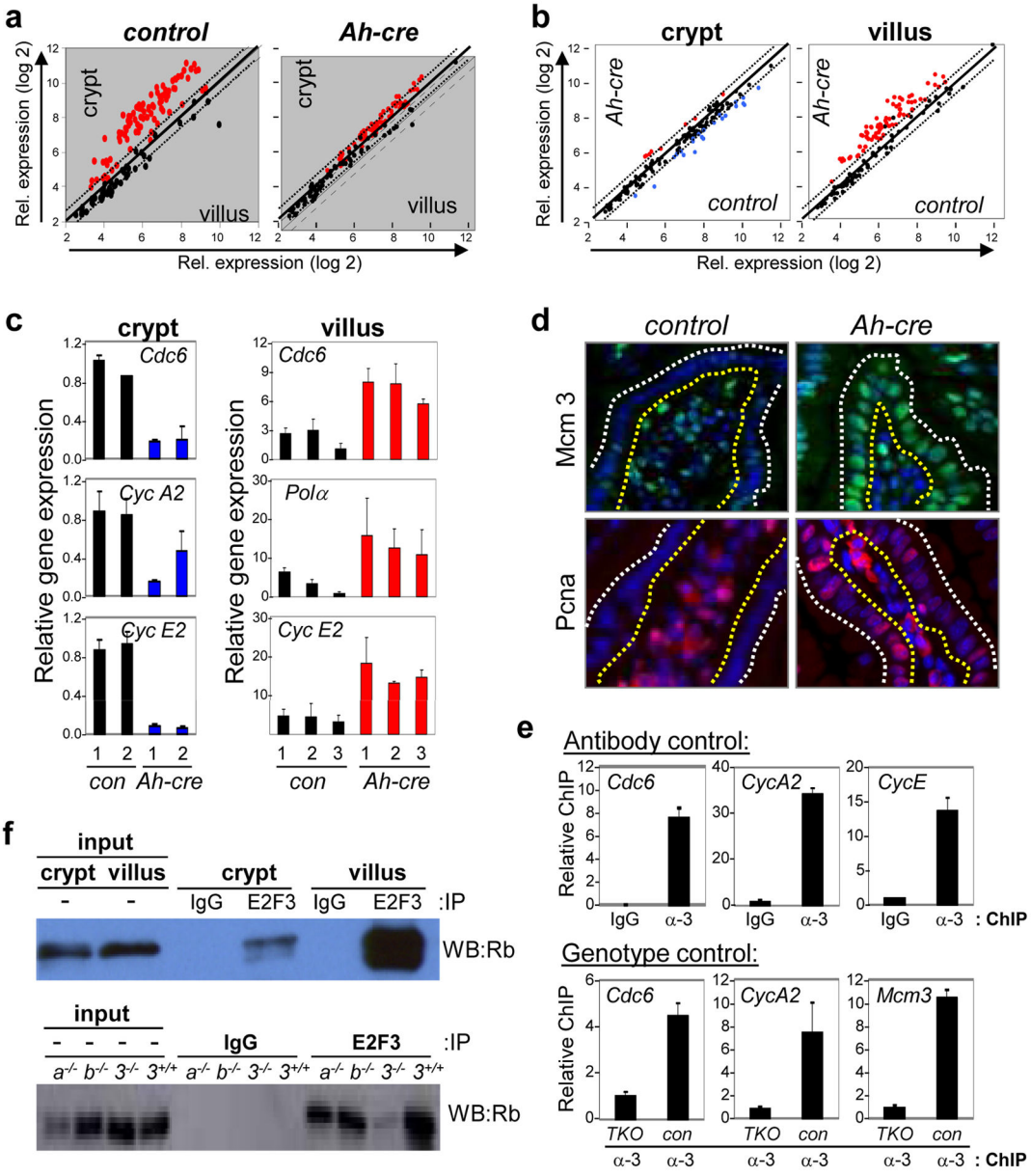

Figure 3. Repression of E2F-target genes in *E2f1-3* deficient villi

a Scatter plots comparing expression of known E2F-target genes (see Supplementary Fig. 16b) between cell compartments (crypt and villus); $E2f1^{-/-};E2f2^{-/-};E2f3^{LoxP/LoxP}$ (*control*) and *Ah-cre*;$E2f1^{-/-};E2f2^{-/-};E2f3^{LoxP/LoxP}$ (*Ah-cre*). Genes with >1.5-fold increase in expression are depicted as red dots. **b.** Scatter plots comparing expression of known E2F-target genes between genotypes (*control* and *Ah-cre* samples); n=3 for each of the four samples. Red dots indicate genes whose expression increased >1.5-fold and blue dots indicate genes that decreased >1.5-fold. **c.** Quantitative real-time PCR was performed to compare the relative expression of selected E2F-target genes in *control* and *Ah-cre* crypts (left panels) and villi (right panels) using specific primers (Supplementary Fig. 20). **d**. Immunohistochemical staining of Mcm3 (green) and Pcna (red) in *control* and *Ah-cre* villi.

DAPI (blue) was used for staining nuclei. Yellow dotted line outlines the luminal side of the villus; white dotted line outlines the outer side of the villus. Note that staining of blood cells in lumens of villi is non-specific. **e**. Chromatin immunoprecipitation (ChIP) assays using IgG or anti-E2F3 (α-3) antibodies with lysates from *wild-type* villi (Antibody control; top panels). ChIP assays using anti-E2F3 (α-3) antibodies with lysates from *wild type* (*con*) and *Ah-cre* (*TKO*) villi (Genotype control: bottom panels). Primers flanking known E2F-binding elements were used to detect the indicated gene promoters (Supplementary Fig. 19). **f.** Co-immunoprecipitation assays of cell extracts prepared from *control* villi and crypts. Imunoprecipitations (IP) used anti-E2F3 antibody or IgG. Anti-Rb antibody was used to probe Western blot (WB; left panel). The specificity of the anti-E2F3 antibody used in the left panel was evaluated in intestinal lysates derived from *Ah-cre* ($3^{-/-}$), *E2f3a*$^{-/-}$ ($3a^{-/-}$), *E2f3b*$^{-/-}$ ($3b^{-/-}$) and *E2f3*$^{+/+}$ mice. Anti-Rb antibody was used to probe Western blot (WB; right panel).

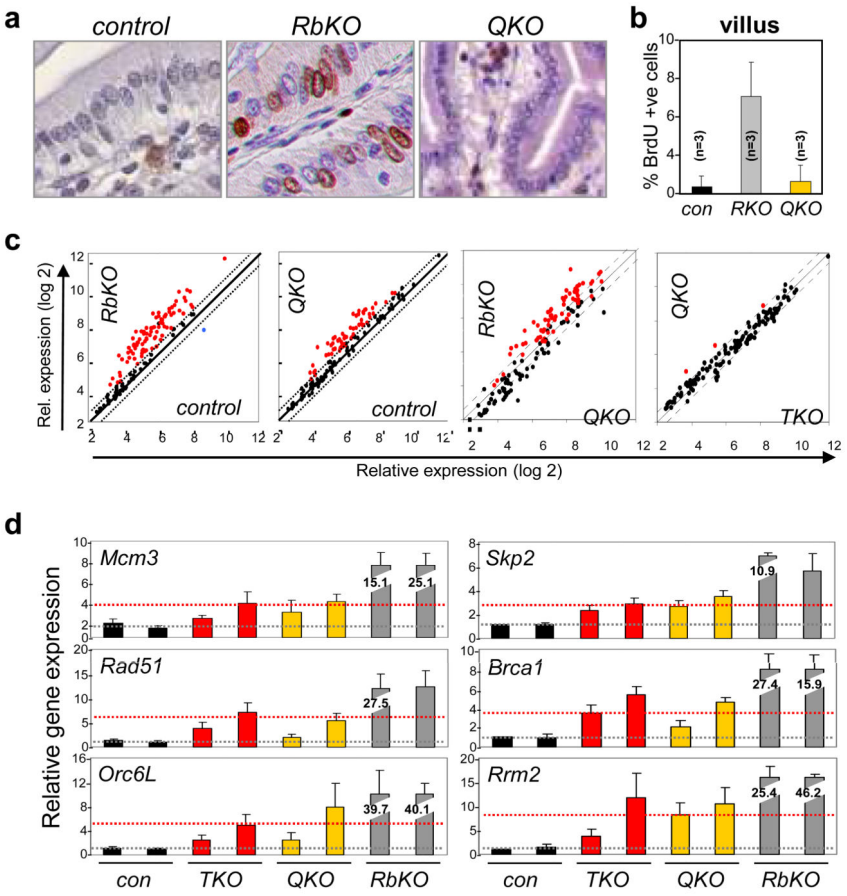

Figure 4. E2F1-3 contribute to the ectopic cell proliferation caused by *Rb*-deficiency

a BrdU analysis was performed in *E2f1*$^{-/-}$;*E2f2*$^{-/-}$;*E2f3*$^{LoxP/LoxP}$ (*control*), *Ah-cre;Rb*$^{LoxP/LoxP}$ (*RbKO*) and *Ah-cre;E2f1*$^{-/-}$;*E2f2*$^{-/-}$;*E2f3*$^{LoxP/LoxP}$;*Rb*$^{LoxP/LoxP}$ (*QKO*) small intestines. **b.** Quantification of BrdU incorporation. n=3, 3 different animals with the indicated genotypes were analyzed; error bars indicate standard deviation. **c.** Scatter plot analysis comparing differentially expressed E2F target genes in *control*, *RbKO*, *Ah-cre;E2f1*$^{-/-}$;*E2f2*$^{-/-}$;*E2f3*$^{LoxP/LoxP}$ (*TKO*) and *QKO* villi; n=3 for each of the eight samples. Red dots indicate genes whose expression increased >1.5-fold and blue dots indicate gene that decreased >1.5-fold. **d.** Quantitative RT-PCR analysis of selected E2F-target genes in *control (con)*, *RbKO*, *TKO*, and *QKO* villi. The normal basal level of E2F target expression is illustrated as a grey dotted line and the threshold level of E2F target expression required for ectopic proliferation is illustrated as a red dotted line.